THE JOURNAL OF BIOLOGICAL CHEMISTRY VOL. 284, NO. 31, pp. 20858–20868, July 31, 2009

An Essential Role for the *Plasmodium* Nek-2 Nima-related Protein Kinase in the Sexual Development of Malaria Parasites*

Received for publication, February 17, 2009, and in revised form, May 8, 2009 Published, JBC Papers in Press, June 2, 2009, DOI 10.1074/jbc.M109.017988

Luc Reininger[‡1], Rita Tewari[§¶1,2], Clare Fennell[‡3], Zoe Holland[‡3], Dean Goldring[‖], Lisa Ranford-Cartwright[**], Oliver Billker[¶‡‡], and Christian Doerig[‡§§4]

From the [‡]INSERM U609-Wellcome Centre for Molecular Parasitology, Biomedical Research Centre, and [**]Division of Infection and Immunity, Faculty of Biomedical and Life Sciences, University of Glasgow, 120 University Place, Glasgow G12 8TA, Scotland, United Kingdom, the [§]Institute of Genetics, School of Biology, University of Nottingham, Nottingham NG72UH, United Kingdom, the [‖]Department of Biochemistry, School of Biochemistry, Genetics Microbiology and Plant Pathology, University of KwaZulu-Natal, Scottsville 3209, South Africa, the [‡‡]Wellcome Trust Sanger Institute, Hinxton, Cambridge CB10 1SA, United Kingdom, the [¶]Division of Cell and Molecular Biology, Imperial College London, London SW7 2AZ, United Kingdom, and [§§]INSERM U609, Global Health Institute, Ecole Polytechnique Fédérale de Lausanne (EPFL), Station 19, CH-1015 Lausanne, Switzerland

The molecular control of cell division and development in malaria parasites is far from understood. We previously showed that a *Plasmodium* gametocyte-specific NIMA-related protein kinase, nek-4, is required for completion of meiosis in the ookinete, the motile form that develops from the zygote in the mosquito vector. Here, we show that another NIMA-related kinase, Pfnek-2, is also predominantly expressed in gametocytes, and that Pfnek-2 is an active enzyme displaying an *in vitro* substrate preference distinct from that of Pfnek-4. A functional *nek-2* gene is required for transmission of both *Plasmodium falciparum* and the rodent malaria parasite *Plasmodium berghei* to the mosquito vector, which is explained by the observation that disruption of the *nek-2* gene in *P. berghei* causes dysregulation of DNA replication during meiosis and blocks ookinete development. This has implications (i) in our understanding of sexual development of malaria parasites and (ii) in the context of control strategies aimed at interfering with malaria transmission.

Malaria, caused by infection with intracellular protozoan parasites of the genus *Plasmodium*, is a major public health problem in the developing world (1). The species responsible for the vast majority of lethal cases is *Plasmodium falciparum*. The life cycle of malaria parasites consists of a succession of developmental stages: asexual multiplication occurs in the human host (first in a single round of schizogony in a hepatocyte infected by a sporozoite injected by the mosquito vector, and then multiple rounds of schizogony in erythrocytes), whereas the sexual cycle is initiated by the formation of cell cycle-arrested gametocytes in infected erythrocytes and proceeds, in the midgut of the mosquito vector, to gametogenesis, fertilization, and formation of a motile ookinete. The ookinete crosses the midgut epithelium and establishes an oocyst at the basal lamina, in which sporogony occurs, generating sporozoites that render the vector infectious once they reach its salivary glands. The alternation of proliferative and non-proliferative phases implies that the control of cell cycle progression is of prime importance for completion of the life cycle of the parasite.

The NIMA-related protein kinases (Neks)[5] constitute an extended family of eukaryotic mitotic serine/threonine kinases. The best characterized members of the Nek family include NIMA (never in mitosis/*Aspergillus*), the founding member from the fungus *Aspergillus nidulans* (2), and its closest homologue in mammals, Nek2 (3, 4). Initially identified as a kinase essential for mitotic entry in *Aspergillus*, NIMA has been also shown to participate in nuclear membrane fission (5). Eleven members of the NIMA kinase family (Nek1–11) have now been identified in various human tissues, and together fulfill a number of cell cycle-related functions in centrosome separation, mitosis, meiosis, and checkpoint control (reviewed in Ref. 6). It has been proposed that expansion of the Nek family accompanied the evolution of a complex system for the coordination of progression through the cell cycle with the replication of cellular components such as cilia, basal bodies, and centrioles. Sev-

* Work at the *Plasmodium* Genome Consortium was supported by the Burroughs Wellcome Fund, the Wellcome Trust, the National Institutes of Health (NIAID), and the U.S. Department of Defense, Military Infectious Diseases Research Program. Financial support for PlasmoDB was provided by the Burroughs Wellcome Fund. Work in the laboratory of C. D. was supported by the French Institut National de la Santé et de la Recherche Médicale (Inserm), FP6 (SIGMAL and ANTIMAL projects, BioMalPar Network of Excellence) and FP7 (MALSIG project) programs of the European Commission, and by a grant from the Novartis Institute for Tropical Diseases (NITD, Singapore). The work on *P. berghei* was supported by grants from the Wellcome Trust (to R. T. and O.B.) and the Medical Research Council (to O. B.).

⌘ *Author's Choice*—Final version full access.

[1] Both authors contributed equally to this work.

[2] To whom correspondence may be addressed: Institute of Genetics, School of Biology, University of Nottingham, Nottingham NG7 2UH, United Kingdom. Tel.: 44-115-8230362; Fax: 44-115-8230338; E-mail: rita.tewari@nottingham.ac.uk.

[3] Recipients of Ph.D. studentships awarded by the Wellcome Trust.

[4] To whom correspondence may be addressed: INSERM U609, Wellcome Centre for Molecular Parasitology, Global Health Institute, Ecole Polytechnique Fédérale de Lausanne (EPFL), Station 19, CH-1015 Lausanne, Switzerland. Tel.: 41-21-693-0983; Fax: 41-21-693-9538; E-mail: christian.doerig@epfl.ch.

[5] The abbreviations used are: Nek, NIMA-related protein kinases; RT, reverse transcriptase; MAPK, mitogen-activated protein kinase; GFP, green fluorescent protein; RT, reverse transcriptase; DHFR, dihydrofolate reductase; TRITC, tetramethylrhodamine isothiocyanate; UTR, untranslated region; GST, glutathione *S*-transferase; MBP, myelin basic protein.

eral human Neks have C-terminal extensions to their catalytic domain, which contain regulatory elements (*e.g.* PEST sequences that function as target for cell cycle-dependent proteolytic degradation, or coiled-coil domains mediating dimerization). Nek6 and Nek7 have no large extensions, but bind to the C-terminal non-catalytic tail of Nek9, an enzyme that becomes activated during mitosis and is likely to be responsible for the activation of Nek6 (7). This may represent a novel cascade of mitotic NIMA family protein kinases whose combined function is important for mitotic progression.

The *P. falciparum* kinome includes four NIMA-related serine/threonine kinases (8). Pfnek-1 (PlasmoDB identifier PFL1370w) clusters within the *Aspergillus* NIMA/human Nek2 branch in phylogenetic trees, whereas clear orthology to mammalian or yeast Neks could not be assigned for the three other *P. falciparum* sequences (Pfnek-2, -3, and -4, PlasmoDB identifiers PFE1290w, PFL0080c, and MAL7P1.100, respectively) (9). Microarray data (10) available in the PlasmoDB data base (11) indicate that Pfnek-1 is expressed in asexual and sexual stages, whereas mRNA encoding the other three enzymes is predominantly or exclusively expressed in gametocytes, suggesting a possible role in the sexual development of the parasite. Consistent with this hypothesis, we previously showed that rodent malaria parasites *Plasmodium berghei* lacking the Nek-4 enzyme are unable to complete DNA replication to 4C in the zygote prior to meiosis (9). Pfnek-1, -3, and -4 have been characterized at the biochemical level and are active as recombinant enzymes (9, 12, 13). Pfnek-1 and Pfnek-3 have surprisingly been implicated as possible regulators of an atypical mitogen-activated protein kinase (MAPK), as both enzymes synergize with the Pfmap-2 MAPK *in vitro* (12, 13); the physiological relevance of these observations remains to be demonstrated.

Here, we demonstrate that Pfnek-2, like the other three members of the *P. falciparum* Nek family, is a *bona fide* protein kinase. Analysis of the expression pattern demonstrates that low levels of Pfnek-2 mRNA are actually detectable in asexual parasites, even though transgenic parasites expressing a green fluorescent protein (GFP)-tagged Pfnek-2 under the control of its cognate promoter display female gametocyte-specific expression. To investigate the function of this kinase, parasite clones with a disrupted *nek-2* gene were generated in *P. falciparum* and *P. berghei;* transmission experiments identified an important role for nek-2 in sexual development: *nek-2*$^{-}$ parasites are able to differentiate into mature gametocytes and to undergo gametogenesis, but do not develop into ookinetes. Further investigations on the *pbnek-2*$^{-}$ parasites showed that pre-meiotic DNA replication is dysregulated in the mutant clones.

EXPERIMENTAL PROCEDURES

Molecular Cloning, Expression, and Kinase Assays of Pfnek-2—Oligonucleotides (forward, OL10 GGGGGATCCATGTCTAAACCCAAAATG; reverse, OL9 GGGGGTCGACTCAAATTTGGCTATTCCT) were designed to contain the start and stop codons of the full-length, 8-exon Pfnek-2 open reading frame combining the prediction by the Glimmer algorithm and Pf annotation on PlasmoDB (gene identifier PFE1290w), as well as BamHI and SalI restriction sites (underlined), respectively. The open reading frame was amplified from a gametocyte cDNA library (a gift from Pietro Alano) and the 883-bp amplified product was inserted between the BamHI and SalI sites of the pGEX-4T3 vector yielding the plasmid pGEX-Pfnek-2. Catalytically inactive recombinant pGEX-K38M-Pfnek-2 was obtained by site-directed mutagenesis using the overlap extension PCR technique. A similar strategy was used to generate pGEX-T169A-Pfnek-2 mutant. All inserts were verified by DNA sequencing prior to expression of the recombinant proteins in *Escherichia coli* (strain BL21-CodonPlus). Briefly, cells were grown at 37 °C until an A_{600} of 0.6 was reached, at which time expression of Pfnek-2 was induced by the addition of 0.2 mM isopropyl β-D-galactoside. Expression was induced for 3 h and then harvested by centrifugation. Purification of wild-type and mutated GST-Pfnek-2 was performed following published procedures (9). SDS-PAGE analysis of purified GST-Pfnek-2 revealed a band corresponding to 59 kDa, the predicted molecular mass of the GST-Pfnek-2 fusion protein. Kinase assays were performed in a standard reaction (30 μl) containing 25 mM Tris-HCl, pH 7.5, 15 mM $MgCl_2$, 2 mM $MnCl_2$, 15 mM ATP, 5 μCi of [γ-^{32}P]ATP (3000 Ci/mmol, Amersham Biosciences), and 5 μg of substrate (β-casein, myelin basic protein (MBP), or histone H1 (purchased from Sigma)). Reactions were initiated by the addition of 1 μg of the recombinant wild-type or mutated Pfnek-2. The reaction proceeded for 30 min at 30 °C and was stopped by the addition of Laemmli buffer, boiled for 3 min, and analyzed by electrophoresis on 12% SDS-polyacrylamide gel. The gels were dried and submitted to autoradiography.

P. falciparum Cultures—Asexual stages of the 3D7 clone of *P. falciparum*, its F12 subclone, and the 3D7 transfectants described in this paper were grown in human erythrocytes as described previously using Albumax I instead of human serum (14). Gametocytes were prepared according to the protocol of Carter *et al.* (15). Parasites were released from infected erythrocytes by saponin (0.1% w/v) lysis, washed in phosphate-buffered saline, pH 7.5, and kept frozen at −80 °C until use.

RT-PCR—Total RNA samples were extracted from parasite pellets using TRIzol lysis solution (Invitrogen). DNase treatment of RNA samples prior to RT-PCR was performed by incubation at 37 °C for 30 min using the RQ1 RNase-free DNase purchased from Promega. The DNase was inactivated by incubation at 65 °C for 10 min. RT-PCRs were performed with 500 ng of total RNA/reaction using the ImPromII reverse transcription system purchased from Promega. In control reactions reverse transcriptase was omitted, and only *Taq* polymerase (TaKaRa) was present. The RT reactions were incubated at 42 °C for 1 h. For the PCR (30 cycles at 94 °C for 45 s, 55 °C for 45 s, and 68 °C for 2 min 30 s), Pfnek-2-specific primers were the forward OL10 and reverse OL9 oligonucleotides described above used for the cloning and expression of the full-length Pfnek-2 open reading frame. For nested PCR (25 cycles at 94 °C for 45 s, 55 °C for 45 s, and 68 °C for 2 min), 1 μl (1/25) of each PCR product was reamplified using the Pfnek-2-specific primers forward OL42 and reverse OL43 oligonucleotides used for construction of the knock-out plasmid described below. Products of both series of reactions were resolved on a 1% agarose gel.

Generation of P. falciparum Transgenic Parasites—The Pfnek-2 disruption plasmid (pCAM-Pfnek-2) was generated by inserting a PCR product corresponding to a central portion of the catalytic domain of the enzyme into the pCAM-BSD vector (a gift from David Fidock), which contains a cassette conferring resistance to blasticidin. The insert was obtained using 3D7 genomic DNA as template and the following oligonucleotides: forward, OL42 GGGGGGATCCTCGTTTGGAATTGTAACTGC; reverse, OL43 GGGGCGGCCGCTGGTGCCATATATCCTA, which contain BamHI and NotI sites (underlined), respectively.

The Pfnek-2-GFP plasmid (pCHD-Pfnek-2) was generated by using the pHGB and pCHD-1/2 transfection vectors based on Gateway™ recombinational cloning established by Tonkin *et al.* (16). The ~1-kb 5′-flanking region of Pfnek-2 was amplified from 3D7 genomic DNA using the forward (GGGTCGACCTATTAGGAAATATGAAG) and reverse (CCAGATCTACTAATATGATTATTCATAC) oligonucleotides containing SalI and BglII sites (underlined), respectively, and inserted into the SalI/BglII sites of pHGB to produce the plasmid pHGB-Pfnek-2 5′. We next amplified the Pfnek-2 open reading frame from the gametocyte cDNA library indicated above and the oligonucleotides forward, CCCAGATCTATGTCTAAACCCAAAATGATAG and reverse, CCCCCTAGGAATTTGGCTATTCCTTTCTTGC, containing BglII and AvrII sites (underlined), respectively. The digested product was ligated into the BglII/AvrII sites of plasmid pHGB-Pfnek-2 5′ to produce the pHGB-Pfnek-2 entry clone. This plasmid was used in a recombination reaction with the pCHD-1/2 destination vector containing the cassette responsible for expression of hDHFR, the gene mediating resistance to WR99210 treatment, to produce the final transfection vector pCHD-Pfnek-2. pCHD-Pfnek-2 contains the full-length Pfnek-2 coding sequence in-frame with the downstream fluorescent reporter GFP gene, driven by its own 5′ promoter region and terminated by the *P. berghei* DHFR-TS 3′ terminator.

Transfections were carried out by electroporation of ring stage 3D7 parasites with 50–100 μg of plasmid DNA, according to Sidhu *et al.* (17). Blasticidin (Calbiochem) or WR99210 (Jacobus Pharmaceutical Co., Inc., Princeton, NJ) were added to a final concentration of 2.5 μg/ml and 5 nM, respectively, 48 h after transfection to select for transformed parasites. Resistant parasites appeared after 3–4 weeks and were maintained under drug selection. Subsequent to genotyping indicating that integration occurred at the target locus, Pfnek-2 knock-out parasites were cloned by limiting dilution in 96-well plates for further genotypic and phenotypic analyses.

Genotype Analysis of pfnek-2$^-$ Parasites—Genotypes of Pfnek-2 knock-out parasites were analyzed by PCR and Southern blotting, using standard procedures. Genomic DNA from transfectants and 3D7 control parasites were extracted from frozen saponin lysis pellets by standard proteinase K digestion in the presence of SDS, phenol/chloroform/isoamyl alcohol (24:24:1) extraction, and ethanol precipitation. Genomic DNA pellets were resuspended in 10 mM Tris-HCl, pH 8.0, 1 mM EDTA (TE) buffer prior to analysis. Disruption of the Pfnek-2 locus was analyzed by diagnostic PCR using various primer pairs. The primer pair OL10/OL9 produced a 1.8-kb fragment corresponding to the undisrupted Pfnek-2 locus only with template from wild-type 3D7. The primer pair OL167 (TATTCCTAATCATGTAAATCTTAAA) and OL168 (CAATTAACCCTCACTAAAG) specific for the pCam-BSD vector, produced a 1.4-kb fragment corresponding to the episome only in pCAM-Pfnek-2 transfectants. Primer pairs OL10/OL168 and OL167/OL9 amplified across the 5′ and 3′ ends of the integration site, giving rise to 1.3- and 1.9-kb products only in the disrupted locus, respectively. For Southern blot analysis, 5 μg of genomic DNA was digested with EcoRI, separated on a 0.7% agarose gel and transferred to Hybond N+ membrane according to the manufacturer's procedures (Amersham Biosciences). The blot was probed with the fluorescein isothiocyanate-labeled Pfnek-2 sequence amplified from 3D7 genomic DNA with the primer pair OL42/OL43 (used to produce the Pfnek-2 knock-out construct), and incubated with an anti-fluorescein isothiocyanate monoclonal antibody conjugated to horseradish peroxidase purchased from Amersham Biosciences. Chemoluminescence detection was performed using the Western Lightning Chemoluminescence Reagent Plus detection kit (PerkinElmer) and exposure to imaging Hyperfilm MP (Amersham Biosciences).

Microscopy—Parasites expressing GFP were fixed with methanol. Images were captured using a Delta vision deconvolution fluorescence microscope (×100 objective Olympus IX-70) after counterstaining (i) with a rat anti-Pfg377 antibody (a kind gift from Pietro Alano), using a red Alexa Fluor 594-conjugated rabbit anti-rat IgG (H+L) secondary antibody and (ii) with 4′,6-diamidino-2-phenylindole. The pattern of microtubules in gametocytes was determined on methanol-fixed parasites stained with a mouse monoclonal antibody specific for chick brain α-tubulin (clone DM1A, purchased from Sigma) and a secondary TRITC-labeled goat anti-mouse IgG (Southern Biotech, Birmingham, AL).

Western Blotting—Western blot analysis was performed on cell-free extracts prepared by resuspending parasite pellets in phosphate-buffered saline containing 0.1% SDS, 0.05% sodium deoxycholate, 1 mM phenylmethylsulfonyl fluoride, and Complex™ mixture protease inhibitor tablet from Roche Applied Science. 10 μg of each extract were boiled in Laemmli sample buffer, separated on 12% SDS-polyacrylamide gels, and subsequently electrotransferred to nitrocellulose membranes (Bio-Rad). Membranes were blocked in 5% skim milk and Tris-buffered saline containing 0.05% Tween 20 overnight at 4 °C. Immunoblotting was performed using mouse monoclonal anti-GFP antibody (1:5000 dilution) (Roche) and horseradish peroxidase-conjugated sheep anti-mouse antiserum (1/10 000 dilution) (Sigma). Bound antibodies were detected using Western Lightning Chemiluminescence Reagent Plus detection kit (PerkinElmer) and exposure to imaging hyperfilm MP (Amersham Biosciences).

Mosquito Infection with P. falciparum—Gametocytes of each parasite clone were grown *in vitro* and fed to *Anopheles gambiae* mosquitoes through membrane feeders as described previously (15), using medium containing 10% human serum instead of Albumax. Mosquitoes were dissected at 48 h or 10 days post-infection for microscopic analysis of ookinete formation and oocyst infection of the midgut, respectively.

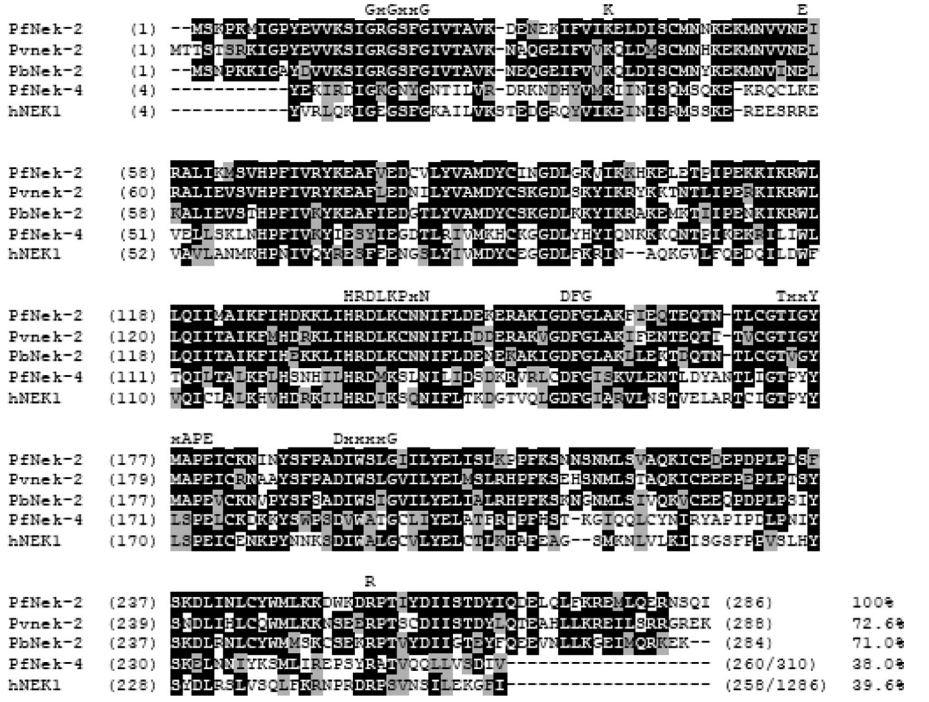

FIGURE 1. **Alignment of the amino acid sequence of Pfnek-2 with that of other NIMA-related protein kinases.** Sequences used are: full-length sequence of *Plasmodium vivax* and *P. berghei* orthologues, Pvnek-2 (Pv079950) and Pbnek-2 (PB000208.03.0); catalytic domains of *P. falciparum* Pfnek-4 (MAL7P1.100) and human NEK1 (SwissProt Q96PY6). Sequences were aligned using CLUSTAL W. Identical amino acids are *shaded in black* and similar amino acids in *gray*. The signature of Ser/Thr protein kinases is added *above* the sequences. Thr[169] is indicated with an *asterisk*. The percentage of identity to Pfnek-2 is shown at the *end* of each sequence.

Generation of pbnek-2⁻ Parasite Clones—pbnek-2⁻ P. berghei (ANKA) parasites were generated by double homologous recombination using the targeting vector pBSDHFR, in which the *Toxoplasma gondii* dihydrofolate reductase/thymidylate synthase gene (DHFR/TS) is flanked by the upstream and downstream control elements from *P. berghei* DHFR/TS. A 776-bp fragment of the 5′ UTR of the *pbnek-2* gene was amplified from genomic DNA using the following primers (restriction sites are underlined): forward (K0071), GGGGGGTACC-TTGGTTCAAAATCATACATAATG; reverse (K0072), GGG-GGGGGCCCTGCCATTCTTCAATGACTTAT. The amplicon was inserted into pBSDHFR as a KpnI/ApaI fragment upstream of the DHFR/TS cassette. 550 bp of the *pbnek-2* 3′ UTR were then amplified from genomic DNA using the following primers: forward (K0073), GGGGGGATCCGCCTGATCCACTTC-CTAGTA; reverse (K0074), GGGGCCGCGGATTCAATG-GACGGACGC. The amplicon was inserted as a BamHI/SacII fragment downstream of the DHFR/TS cassette. The final construct was digested with KpnI and SacII to excise the fragment prior to transfection into *P. berghei*. A second independent *pbnek-2⁻* clone was generated in *P. berghei* ANKA clone 507 expressing GFP (18). The pyrimethamine-resistant parasites were then cloned by limiting dilution and two independent clones (one from each transfection) were genotyped.

Genotype Analysis of pbnek-2⁻ Mutant Parasites—For pulsed field gel electrophoresis, chromosomes of wild-type and *pbnek-2⁻* clones were separated on an LKB 2015 Pulsaphor system using a linear ramp of 60–500 s for 72 h at 4 V/cm. The gel was blotted and hybridized with a probe that binds to the 3′ UTR of DHFR/TS detecting both the endogenous *dhfr* locus (chromosome 7) and the modified *pbnek-2* locus (chromosome 10). For Southern analysis, genomic DNA from wild-type mutant parasites was digested with EcoRI. The fragments were separated on a 0.8% agarose gel, blotted onto a nylon membrane, and probed with the fragment of the *pbnek-2* 3′ UTR used in the knock-out vector (see above).

Phenotypic Analysis of pbnek-2⁻ Parasites—We followed procedures similar to those described earlier (9, 19). In short, gamete activation was triggered by treating the parasite-infected blood with 50 μM xanthurenic acid. Zygote formation and ookinete conversion rates were monitored in *in vitro* cultures by immunolabeling the macrogamete/zygote/ookinete marker P28 as reported earlier (9, 19); Hoechst 33342 was used for nuclear staining. The stained cells were analyzed on a Leica DMR microscope fitted with an Axiovision digital camera. For mosquito transmission triplicate sets of 50–70 *Anopheles stephensi* mosquitoes were allowed to feed on anesthetized infected mice on days 3–4 of blood infection for 30 min at 20 °C.

RESULTS

pfnek-2 Gene Structure—Gene prediction algorithms on PlasmoDB proposed conflicting gene structures for Pfnek-2. To resolve this issue, we amplified, cloned, and sequenced the Pfnek-2 open reading frame from a 3D7 gametocyte cDNA library, using primers hybridizing to the most distal of the predicted START and STOP codons. Sequences obtained from 12 clones concurred to show that the 864-bp Pfnek-2 open reading frame comprises eight exons, a gene structure that differs from all gene predictions proposed in PlasmoDB: exons 1 and 2 follow the "Glimmer" prediction, whereas exons 3–8 are as proposed by the Pf annotation. Translation of the Pfnek-2 open reading frame would generate a 286-amino acid, 33.3-kDa protein with a pI of 7.8 (Fig. 1). The 11 subdomains characteristic of serine/threonine protein kinases, as well as most of the key residues that are largely invariant in this family, are conserved in Pfnek-2. In contrast to most Nek family members, Pfnek-2 has a very short (19 amino acids) C-terminal extension with no identified motifs or domains. However, a possible PEST motif (PESTfind score +7.63), targeting proteins to proteolytic degradation, is found within the catalytic domain. Although some Neks have been reported to oligomerize via a coiled-coil domain present in their C-terminal extension, no such sequence is found within Pfnek-2.

Kinase Activity of Recombinant GST-Pfnek-2—The Pfnek-2 protein was expressed in *E. coli* with an N-terminal GST tag.

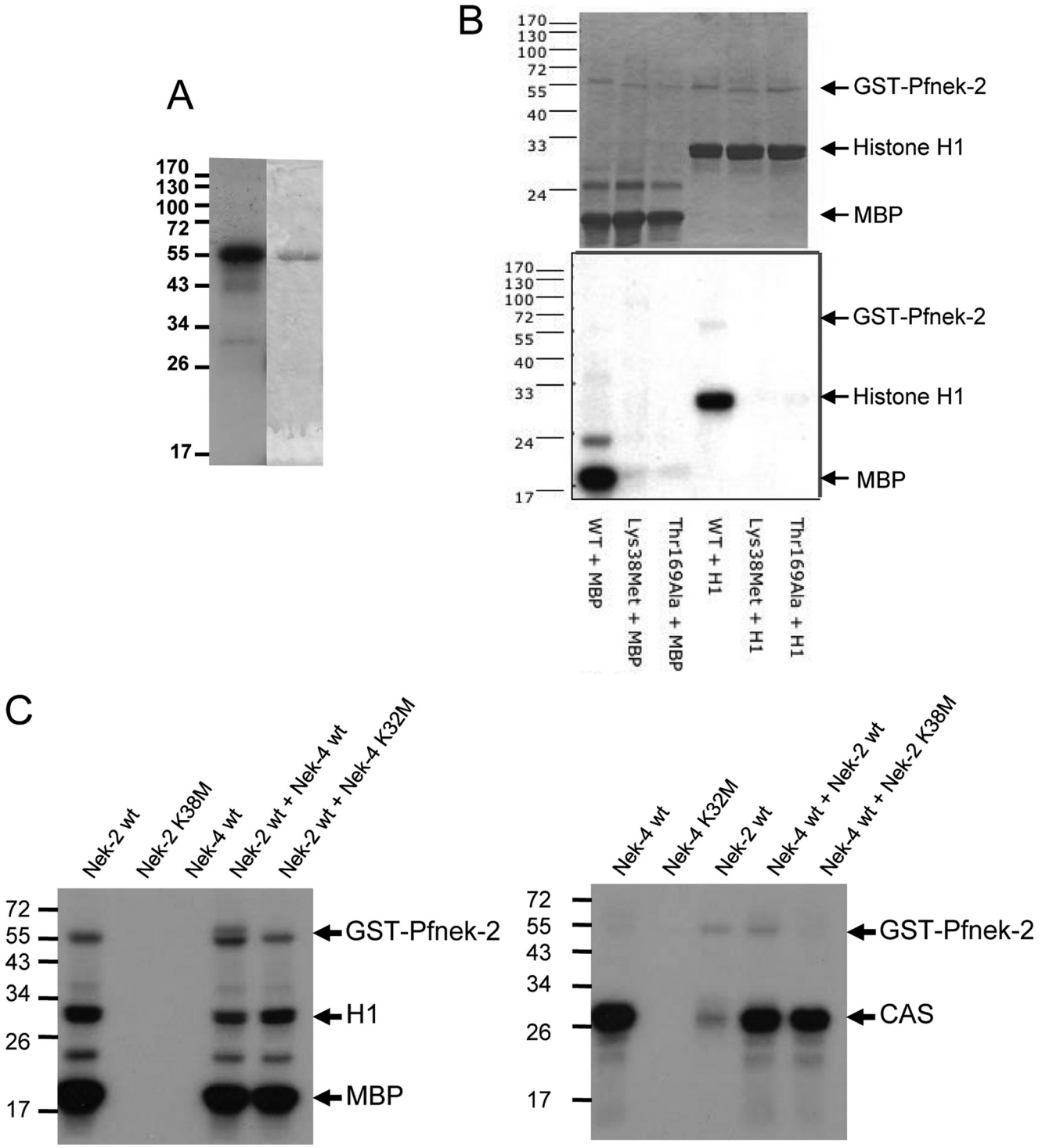

FIGURE 2. **Kinase activity of recombinant Pfnek-2.** *A*, GST-Pfnek-2 autophosphorylation. A kinase assay containing [γ-^{32}P]ATP and 1 μg of wild-type Pfnek-2, without exogenous substrates, was run on an SDS-PAGE, stained with Coomassie Blue, dried, and exposed for autoradiography. *Left*, autoradiogram; *right*, Coomassie Blue-stained gel. *B*, kinase activity of GST-Pfnek-2 toward exogenous substrates. Kinase assays containing [γ-^{32}P]ATP, 1 μg of wild-type GST-Pfnek-2, K38M GST-Pfnek-2 mutant, or T169A GST-Pfnek-2 mutant. MBP and histone H1 (H1) were used as substrates. *Top*, Coomassie Blue-stained gel; *bottom*, autoradiogram. *C*, absence of cross-phosphorylation/activation between GST-Pfnek-2 and GST-Pfnek-4. Autoradiograms for kinase assays containing [γ-^{32}P]ATP, 2.5 μg of wild-type GST-Pfnek-2, K38M GST-Pfnek-2 mutant, wild type GST-Pfnek-4, K32M GST-Pfnek-4 mutant, and combinations of GST-recombinant fusion proteins toward exogenous substrates. MBP and H1 (*left panel*) and dephosphorylated caseine (*CAS*) (*right panel*) were used as substrates. GST-Pfnek-2 autophosphorylation is indicated.

Purified recombinant GST-Pfnek-2 possessed kinase activity, as demonstrated by its ability to autophosphorylate (Fig. 2*A*) and to phosphorylate exogenous substrates such as myelin basic protein (MBP), histone H1 (Fig. 2*B*), and β-casein (data not shown). To verify whether the activity was indeed due to GST-Pfnek-2 rather than to a co-purifying contaminant, we showed that a catalytically inactive mutant enzyme (Lys^{38} $\rightarrow$ Met) did not yield any signal in the phosphorylation assay.

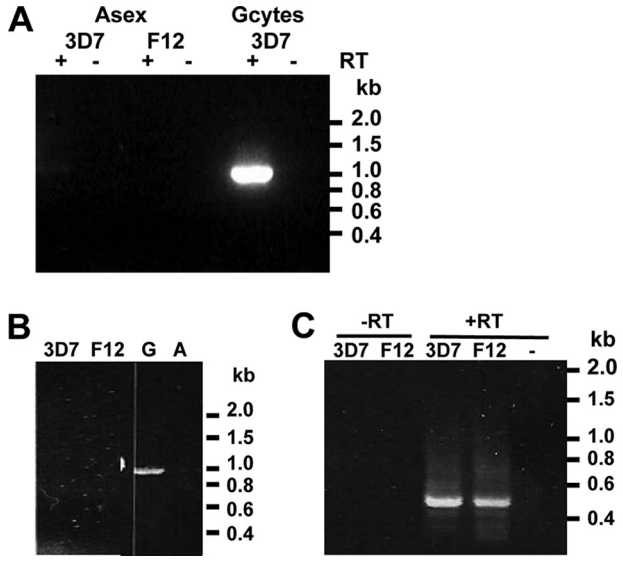

FIGURE 3. **Stage specificity of Pfnek-2 mRNA expression.** RT-PCR analysis was performed on total RNA isolated from 3D7, and its gametocyte-less F12 subclone using primers specific for Pfnek-2. *A*, experiment 1, one-step (non-nested) RT-PCR showing detection of Pfnek-2 mRNA in gametocytes, but not asexual blood stages. The lanes labeled − are Pfnek-2 PCR performed in the absence of reverse transcriptase. *B*, experiment 2 confirming the lack of amplification of the Pfnek-2 product in a second sample of 3D7 and F12 asexual blood stages and showing its detection in a cDNA library from gametocytes (*G*) but not in a CDNA from asexual parasites (*A*). *C*, nested PCR (*right panel*) revealing a low level of Pfnek-2 gene expression both in 3D7 and F12 asexual parasites. cDNA libraries from 3D7 asexual blood stages and gametocytes were used as controls; −, water control.

Thus, Pfnek-2 is a genuine protein kinase like Pfnek-4, but displays a different substrate preference (Pfnek-4 is unable to phosphorylate MBP or histone H1 (Fig. 2*C* and Ref. 9). Accordingly, kinase assays using heat-inactivated parasite extracts as substrates consistently display different patterns of phosphorylated proteins depending on whether GST-Pfnek-2 or GST-Pfnek-4 is used in the reaction (data not shown). Thr^{169} is conserved in many protein kinases (including Neks) as the site for activating phosphorylation, and mutant human NEK2 lacking this residue display altered kinase activity (20). Likewise, replacement of this threonine with an alanine ablated Pfnek-2 kinase activity, indicating that the amino acid at this position is crucial to enzyme function and suggesting possible regulation by autophosphorylation; the Thr^{169} residue may also be a target for other upstream kinase(s) *in vivo*; the corresponding residue in Nek6 (Ser^{206}) has been shown to be the target of phosphorylation by Nek9 (7). We did not observe any synergy between the activities of GST-Pfnek-2 and GST-Pfmap-2, as had been observed for Pfnek-1 (12) and Pfnek-3 (13) (data not shown). Kinase assays using wild-type and kinase-dead enzymes performed to detect a possible phosphorylation/activation of recombinant Pfnek-2 by Pfnek-4 (or *vice versa*) did not provide any evidence that such cross-activation occurs, at least *in vitro* (Fig. 2*C*).

Expression Profile of Pfnek-2 in Erythrocytic Stages—Microarray analyses indicate that the Pfnek-2 mRNA is predominantly expressed in gametocytes (10). To confirm gametocyte-specific expression, RT-PCR was performed using RNA isolated from asexual stages and gametocytes of the 3D7 clone (Fig. 3*A*). The presence of an amplicon corresponding to the size of the cDNA demonstrated that Pfnek-2 mRNA is indeed predominantly produced in gametocytes, as confirmed by the observation (Fig. 3*B*) that an amplicon was obtained by PCR from a gametocyte-derived cDNA library, but not from a library obtained from asexual parasites. However, in some experiments a faint signal was also detected in the RNA sample from asexual parasites. This might be due either to low-level expression in asexual parasites, or to the presence of small numbers of gametocytes in the asexual parasite population. To distinguish between these possibilities, we resorted to nested RT-PCR using mRNA from clone F12, a clone derived from 3D7 that has lost the ability to undergo gametocytogenesis and does not express even the earliest markers of sexual development (Fig. 3*C*). Samples from both F12 and 3D7 yielded amplified fragments of the expected size for Pfnek-2 cDNA, the identity of which was verified by cloning and sequencing. Control reactions without reverse transcriptase did not yield any signal. Taken together, these data demonstrate that expression of the *pfnek-2* gene is not strictly gametocyte-specific, and that low mRNA levels are present in asexual parasites. We raised antibodies (chicken IgYs) against Pfnek-2-derived peptides as we had previously done for Pfnek-4 (9). Unfortunately, these antibodies cross-reacted with many proteins in parasite extracts (data not shown) and were not used for further studies; instead we resorted to an *in vivo* tagging approach.

Analysis of Transgenic Parasites Expressing GFP-tagged Pfnek-2—To monitor expression of Pfnek-2 at the protein level, we generated parasite lines expressing Pfnek-2 fused to GFP at the C terminus. The chimeric protein was expressed from an episome under the control of its cognate (Pfnek-2) promoter, using 1 kb of genomic sequence upstream of the translation initiation codon. No significant fluorescence was detectable in asexual parasites, whereas gametocytes displayed bright fluorescence from early to late stages. This is consistent with data regarding mRNA levels (not shown), and indicates that the 1-kb upstream sequence did confer stage-specific regulation. Furthermore, counterstaining gametocytes expressing GFP-tagged Pfnek-2 with an antibody against the female-specific antigen Pfg377 revealed that all (100%) of the green fluorescent parasites were Pfg377-positive, as shown by the well documented punctate pattern of red fluorescence associated with the osmiophilic bodies, to which Pfg377 is known to localize (21–23) (Fig. 4*A*). However, gametocytes that did not fluoresce either in red or green were also present in the population, and were presumably the male gametocytes. This indicates that Pfnek-2 expression is restricted to female gametocytes. The green fluorescence appears to be associated with tubular structures that might be the microtubules spanning the length of the gametocyte (24). This would be in line with the association of Neks with microtubules and microtubule-organizing centers in plants (25) and mammals (reviewed in Ref. 6).

We performed Western blots on parasite-infected erythrocytes using an anti-GFP monoclonal antibody (Fig. 4*B*). Reactivity was observed neither in asexual blood stages of the Pfnek-2-GFP transfectant nor in the untransfected parental line, 3D7. In contrast, gametocytes of the transfected parasites expressed proteins that were resolved as a single band of ~60 kDa, the predicted size of the full-length Pfnek-2-GFP fusion protein,

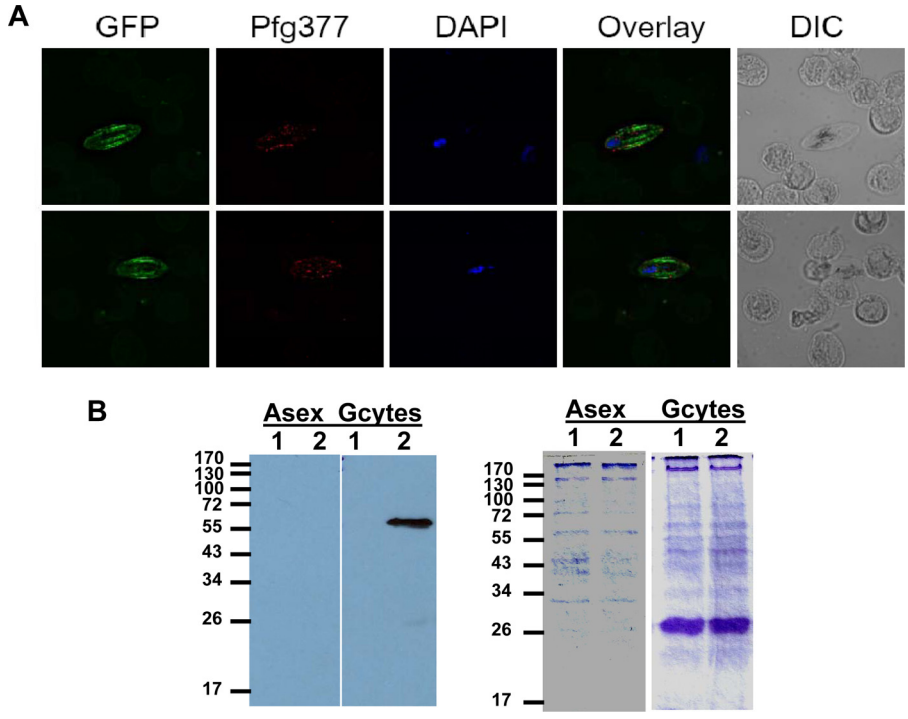

FIGURE 4. **Analysis of GFP in *P. falciparum* gametocytes expressing Pfnek-2-GFP fusion protein.** *A*, fluorescence imaging of two female gametocytes. Images from left to right in each set represent: (i) the fluorescence signal from the GFP protein; (ii) the staining obtained with an anti-Pfg377 antibody (the secondary antibody is conjugated to the Alexa Fluor 594 (*red*)); (iii) 4′,6-diamidino-2-phenylindole (*DAPI*) staining; (iv) an overlay of the former two images; and (v) the DIC image of the cells in the *right panel*. *DIC*, differential interference contrast. *B*, Western blot. 10 μg of parasite cell lysate from asexual stages and stage III–V gametocytes of the 3D7 parental line or Pfnek-2-GFP transfectant were subjected to SDS-PAGE (12% acrylamide), transferred to nitrocellulose membrane, and probed with an anti-GFP antibody (Roche Molecular Biochemicals; 1:5000 dilution). *Left panel*, Western blot; *right panel*, Coomassie Blue-stained SDS-PAGE, stained after transfer. *Lane 1*, 3D7 parental line; *lane 2*, Pfnek-2-GFP transfectant.

showing that the fusion protein is not proteolytically processed and thus validating the live fluorescence imaging.

Nek-2 Is Dispensable for Completion of the Erythrocytic Asexual Cycle and Gametocyte Formation in P. falciparum and P. berghei—To investigate the function of Pfnek-2, we used a reverse genetics approach in which parasite clones with a disrupted *pfnek-2* gene were generated. To this aim, a plasmid based on the pCAM-BSD vector (17), in which the central region of the Pfnek-2 catalytic domain had been inserted next to a cassette conferring resistance to blasticidin, was transferred by electroporation into asexual parasites of the 3D7 clone of *P. falciparum*. After single crossover homologous recombination, neither of the two truncated copies of the pseudo-diploid locus will encode a functional kinase (Fig. 5*A*). Monitoring the blasticidin-resistant population by PCR allowed us to readily detect integration-specific amplicons. To confirm that parasites would be viable despite a disrupted *pfnek-2* gene, we proceeded to clone the transfected population by limiting dilution and to characterize the genotype of individual clones. Two clones, cl.8 and cl.9, obtained from independent transfection experiments were selected for further characterization. PCR analysis showed (i) that these parasites had lost the wild-type gene, (ii) that the episome (or an integrated concatemer) was present in cl.8 but not cl.9, and (iii) that amplicons diagnostic for the 5′ and 3′ boundaries of plasmid integration were produced (Fig. 5*B*). To independently ascertain integration of the pCAM-Pfnek-2 construct at the target locus, we performed a Southern blot (Fig. 5*C*) using EcoRI-digested genomic DNA from wild-type 3D7, cl.8 and cl.9 transfectants, and a Pfnek-2 probe, which gave bands of the expected sizes: the band corresponding to the wild-type locus disappears in the *pfnek-2*$^-$ clones, and is replaced by the two expected bands resulting from integration. In clone c9, the episomal band is readily detectable, indicating that in this clone the episome is retained, or that more than one copy of the knock-out construct is integrated in the locus. Taken together, the PCR and Southern blot analyses show that the Pfnek-2 locus has been disrupted in cl.8 and cl.9. Neither of the *pfnek-2*$^-$ clones was affected in their asexual growth rate *in vitro* (data not shown), and the number, appearance, and sex ratio of gametocytes in the *pfnek-2*$^-$ clones were undistinguishable from those in wild-type parasites, as assessed by examination of Giemsa-stained slides. The association of GFP-Pfnek-2 with microtubular structures (Fig. 4*A*) prompted us to investigate the morphology of microtubules in *pfnek-2*$^-$ gametocytes. Clearly, the mutant gametocytes display normal morphology (Fig. 5*D*). Thus, Pfnek-2 is required neither for erythrocytic schizogony nor for the early stages of the sexual cycle in *P. falciparum*.

To investigate a possible phenotype caused by the absence of a functional Nek-2 enzyme in subsequent stages of the sexual cycle, we resorted to using the *P. berghei*/mouse system, as we did previously with the Nek-4 enzyme (this system is considerably more amenable than *P. falciparum* to this type of studies). The Pbnek-2 protein (PlasmoDB identifier PB000208.03.0) displays 71% identity and 86% similarity to Pfnek-2. The gene was replaced by a DHFR expression cassette conferring resistance to pyrimethamine, using a double cross-over approach (Fig. 6*A*). The pyrimethamine-resistant population was cloned by limiting dilution. Genotype analysis of one of the resulting clones by PCR (not shown), Southern blotting, and pulse-field gel analysis (Fig. 6*B*) indicated that gene replacement had indeed occurred. Two independent clones were generated, one in the wild-type ANKA strain background and the other in an ANKA strain (cl 507) that expresses GFP (18). The asexual cycle of these two clones was then analyzed during infection in mice. No difference in growth rate was observed when compared with wild-type parasites. Furthermore, the *pbnek-2*$^-$ clones produced normal numbers of gametocytes (data not shown). Hence, the *nek-2* gene is dispensable for erythrocytic schizog-

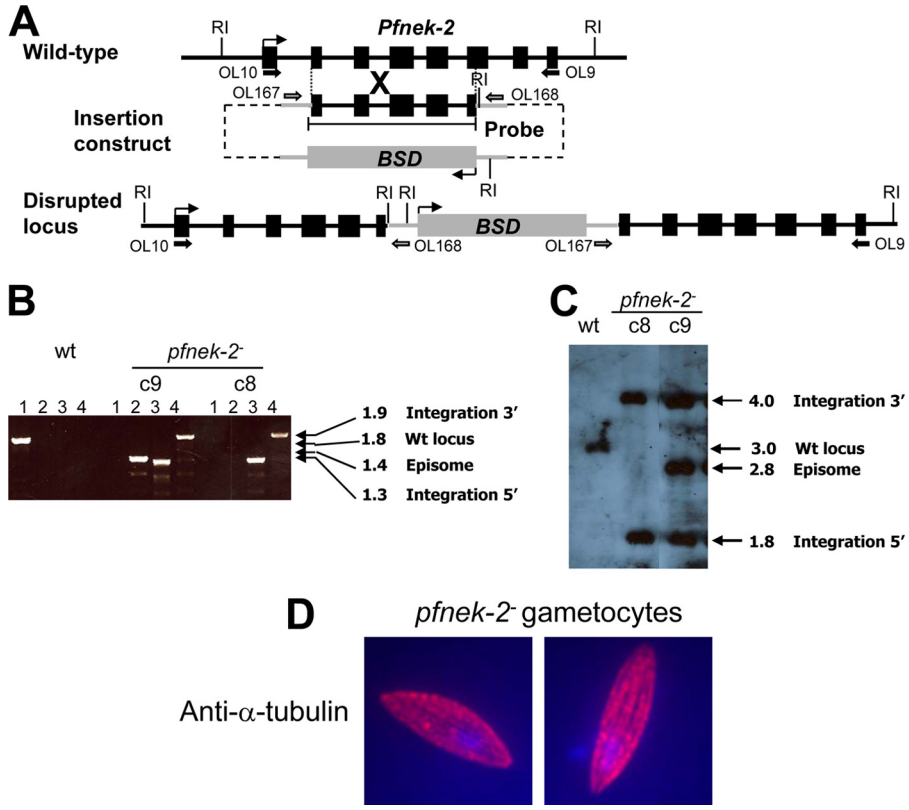

FIGURE 5. **Targeted disruption of the *nek-2* gene in *P. falciparum*.** *A*, strategy for gene disruption. The schematic representation shows the Pfnek-2 locus, the gene-targeting construct used for gene disruption by single homologous recombination, and the pseudo-diploid locus resulting from integration of the knock-out construct. *RI* indicates the location of the EcoRI sites used for Southern blot analysis. The primers used for PCR analysis are indicated. *BSD*, blasticidin-resistance cassette. *B*, PCR indicating disruption of the Pfnek-2 gene in parasite clones cl.8 and cl.9 obtained from two independent transfections. *Lanes 1*, wild-type locus (primers OL10 and OL9); *lanes 2*, episome or concatemers of the knock-out construct (primers OL167 and OL168); *lanes 3*, integration, 5′ boundary (primers OL10 and OL168); *lanes 4*, integration 3′ boundary (primers OL167 and OL9). *C*, Southern blot of genomic DNA from wild-type (*wt*) 3D7, and clones cl.8 and cl.9. Genomic DNA was digested with EcoRI and the blot was hybridized with a DNA probe specific to the region of Pfnek-2 cloned into the knock-out construct. The size in kb and identity of the bands are mentioned to the *right*. *D*, staining of methanol-fixed *pfnek2*$^{-}$ gametocytes with a mouse anti-chicken α-tubulin monoclonal antibody (clone DM1A) and TRITC-labeled goat anti-mouse IgG (H + L) secondary antibody.

ony and gametocytogenesis in both *P. berghei* and *P. falciparum*.

pbnek-2^{-} *Parasites Do Not Develop into Ookinetes and Display Dysregulation of Premeiotic DNA Replication*—The activation of *pbnek-2*$^{-}$ gametocytes after exposure to conditions that trigger gamete formation *in vitro* (26) was then monitored. Microgametocytes were able to exflagellate as efficiently as wild-type parasites (data not shown) and macrogametocytes emerged and rounded normally, as shown by expression of the P28 antigen (Fig. 7*A*). P28 mRNA accumulates in macrogametocytes, but its translation is repressed until gametogenesis occurs, and the protein remains at the cell surface throughout the macrogamete, zygote, and ookinete stages; conversion from zygote to elongated ookinete can be monitored by microscopically assessing cell shape using an anti-P28 antibody. We found that although the total number of P28-expressing parasites was comparable in both *pbnek-2*$^{-}$ clones and wild-type parasites 20–24 h post-activation, the conversion of parasites into banana-shaped ookinetes was abolished in both *pbnek-2*$^{-}$ lines (Fig. 7*B*). Genetic crosses were then used as described previously (9, 19) to determine whether the defect leading to the block in ookinete development was carried by the male or female gametocytes. Crossing *pbnek-2*$^{-}$ with *pbcdpk4*$^{-}$ parasites, in which male gametocyte exflagellation is abolished and which therefore can produce only female gametes (27), restored the ookinete development. This indicates that *pbnek-2*$^{-}$ male gametes are fully functional and can cross-fertilize the *pbcdpk4*$^{-}$ female gametes. In the cross the percentage of females transforming into ookinetes was about half that of wild-type, consistent with *pbnek-2*$^{-}$ female gametes being sterile. In contrast, crossing the *pbnek-2*$^{-}$ clone with a clone lacking Pbnek-4 (in which female gametocytes carry a defect preventing ookinete development (9)) did not restore ookinete conversion capacity (Fig. 8). Thus, absence of Pbnek-2 causes female gametocytes to be unable to support normal development from zygote to ookinete, similar to the developmental phenotype we reported previously for *pbnek-4*$^{-}$ parasites.

To investigate in more detail the stage at which the block in ookinete development occurs, we then quantified the amount of DNA in individual cells using a fluorescent dye. In wild-type parasites, fertilization is followed by fusion of gamete nuclei and one round of replication, increasing the nuclear DNA content of the zygote to 4C prior to meiosis (Fig. 8). Following meiosis four sets of chromosomes are maintained within the nucleus of the ookinete, making this stage tetraploid. *pbnek-2*$^{-}$ parasites appeared to undergo activation and fertilization like wild-type parasites, but fusion of the two nuclei was impaired in a large proportion of the parasites, and the DNA content remained at just above 2C (Fig. 9), a value consistent with the sum of the two gamete nuclei. In all round cells (*i.e.* female gametes, zygotes, and "failed" ookinetes), the DNA content remained below the 4C value expected in normal ookinetes, indicating that the DNA replication process that precedes meiosis is affected in the mutant parasites. This is strikingly similar to the phenotype observed in *pbnek4*$^{-}$ parasites (9). Interestingly, we also observed that about 5% of the *pbnek-2*$^{-}$ P28-positive cells contained an abnormally large amount of DNA, on average 30-fold the haploid amount (Fig. 9), a feature that had not been seen in *pbnek4*$^{-}$ parasites.

The nek-2 Gene Is Essential for Transmission of P. berghei and P. falciparum to the Mosquito—The block in ookinete development *in vitro* suggests that *pbnek-2*$^{-}$ parasites may be unable to establish an infection in the mosquito vector. To verify this, the

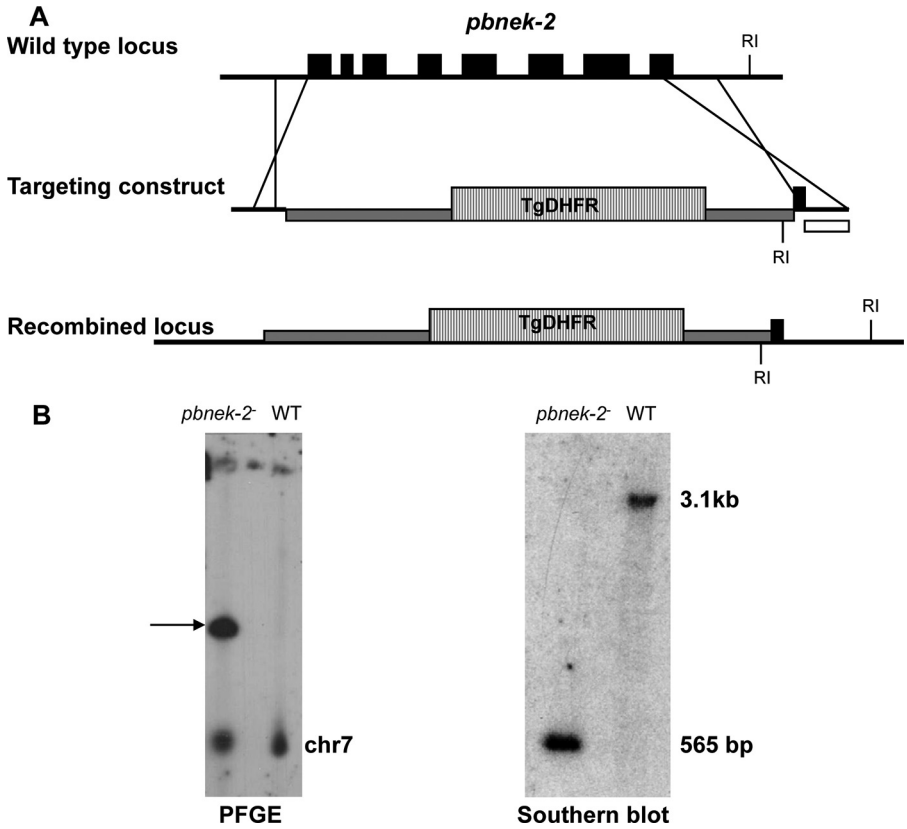

FIGURE 6. **Disruption of the *nek-2* gene in *P. berghei*.** *A*, strategy to disrupt the wild-type (*WT*) *pbnek-2* locus by double crossover homologous recombination. The targeting construct contained a cassette expressing the selectable marker *T. gondii DHFR-TS* (*hatched box*), flanked by the 5′ and 3′ UTRs of the *pbnek-2* gene. *RI* indicates the location of the EcoRI sites used for Southern blot analysis. *B*, genotype analysis. A *pbnek-2*$^-$ clone was analyzed by pulsed field gel electrophoresis using *P. berghei dhfr* 3′ UTR probes that detect both the endogenous *pbdhfr* locus on chromosome 7 and the disrupted *pbnek-2* locus on chromosome 10 (*arrow*). The transgenic clone was also analyzed by Southern blot after digestion of genomic DNA with EcoRI. A probe specific for the *pbnek-2* 3′ UTR (*white box* in *panel A*) was used to detect the expected 3.1-kb fragment in the wild-type and 565-bp fragment in the transgenic parasites.

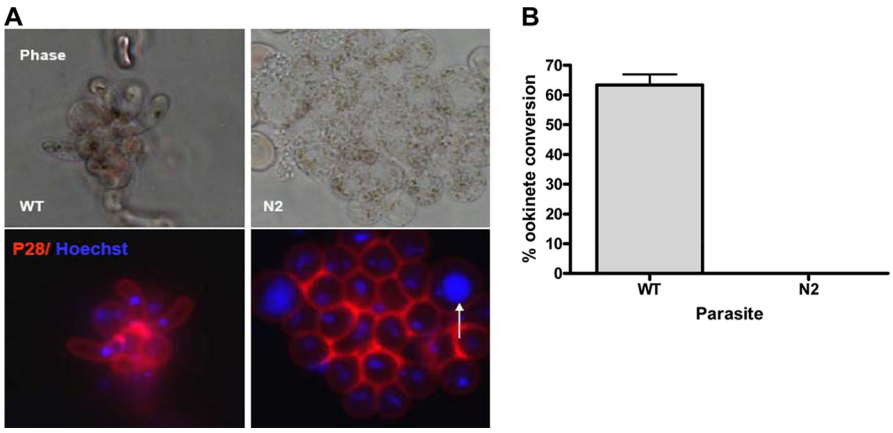

FIGURE 7. **Pbnek-2 is essential for ookinete development and DNA replication in the zygote.** *A*, live parasites from 20–24-h cultures were immunostained with a monoclonal antibody against the female gamete/zygote/ookinete marker P28 (*red*) and counterstained with the nuclear marker Hoechst (*blue*). No ookinetes were detected in the *pbnek-2*$^-$ parasites (*N2*). The presence of 2 nuclei in many cells suggests impairment in nuclear fusion. A small proportion of *pbnek-2*$^-$ cells (*arrow*) showed abnormally elevated DNA content. *B*, quantified ookinete conversion rates for wild-type (*WT*) and the *pbnek-2*$^-$ parasites (*N2*). The histogram displays the percentage of round P28-positive cells adopting the elongated shape of ookinetes. Arithmetic mean ± S.D. from three experiments with parasites from different infected mice are shown.

midguts of *A. stephensi* mosquitoes were examined 10–12 days after the insects had been fed with *pbnek-2*$^-$ or wild-type gametocytes. As shown in Table 1 no oocysts were seen in mosquitoes infected with the knock-out parasite clones, whereas the midguts of mosquitoes infected with wild-type parasite contained 80–100 oocysts. Because disruption of orthologous protein kinase genes can result in different phenotypes in *P. falciparum* and *P. berghei* as seen in case of Pfmap-2 (28), we also proceeded to a similar transmission assay using the *P. falciparum pfnek-2*$^-$ clones. Like the *P. berghei* mutants, the *pfnek-2*$^-$ parasites were unable to produce oocysts in the mosquito (Table 1). This clearly showed that the *nek-2* gene is essential for transmission to the insect vector in both *P. falciparum* and *P. berghei*.

DISCUSSION

Taken together, the phenotypic investigations reported here indicate that parasites lacking Pbnek-2 are unable to properly control premeiotic DNA replication. Murine Nek2 mRNA is present in meiotic tissues with particularly high amounts in testes (29), and the protein associates with meiotic chromosomes (30). In mammals it has been shown that many Nek family members are involved in mitotic progression (31), and human Nek2 is overexpressed in a variety of tumors and may be responsible for defects in chromosome segregation (32). The phenotype of *pbnek2*$^-$ zygotes is thus consistent with Pbnek-2 being involved in functions related to genome replication, similar to Neks in other eukaryotes.

What might be the molecular basis for the meiotic phenotype caused by the lack of Pbnek-2? Our observation (Fig. 4*A*) that the enzyme localizes with what looks like microtubules in female gametocytes is consistent with the established role of Neks in the regulation of microtubule dynamics. An attractive hypothesis to explain the female-carried phenotype in the events that precede meiosis might be that the Nek-2 enzyme, which is present only in female cells, is required for the ontogenesis of the spindles functioning in premeiotic nuclear division. In most animals including humans (33, 34), and in at least some plants

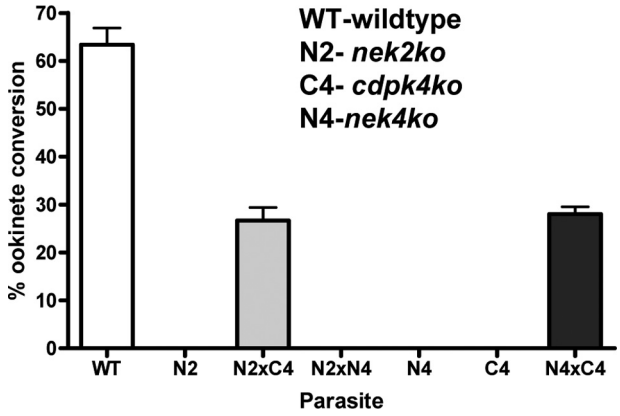

FIGURE 8. **The phenotype of *pbnek-2*$^-$ parasites is carried by macrogametes.** Numbers of ookinetes produced after crossing *pbnek-2*$^-$ (*N2*) with male-defective *pbcdpk4*$^-$ (C4) or female-defective mutant *pbnek-4*$^-$ (*N4*). Wild-type (*WT*) parasites were used as a control for ookinete conversion. The histogram displays the percentage of round P28-positive cells adopting the elongated shape of ookinetes. Arithmetic mean ± S.D. from three experiments with parasites from different infected mice are shown.

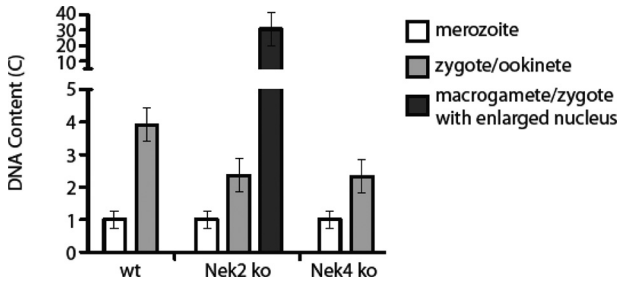

FIGURE 9. **Dysregulation of DNA replication in *pbnek-2*$^-$ parasites.** Nuclear DNA content was measured fluorometrically in Hoechst-stained wild-type and mutant (*pbnek-2*$^-$ and *pbnek-4*) parasite clones. Fluorescence intensity from at least 12 zygote/ookinete nuclei was measured on each slide and normalized to the average signal obtained from the same number of merozoites (haploid, 1C) on the same slide.

(35), the centrioles are paternally inherited, and the same may be true for the centriolar-like structures and microtubule-organizing centers in *Plasmodium*. A possible scenario might thus be that the male-inherited microtubule-organizing centers do not find, in the *nek-2*$^-$ females, the molecular tool that is needed for their development into the meiotic spindle. This could result in a failure of pronuclear fusion and hence the replication step that precedes meiosis, leading to the reduced DNA content we observed. In a minority of *nek-2*$^-$ *P. berghei* zygotes (or possibly unfertilized macrogametes) DNA content appeared to increase unchecked to high levels, a phenomenon not seen in wild-type zygotes and indicating a breakdown of normal cell cycle control in these cells.

The similarity in the phenotypes caused by the loss of Pbnek-2 and Pbnek-4, and the observation (Fig. 2*C*) that the two enzymes do not trans-phosphorylate or -activate *in vitro*, suggest that they function in parallel pathways involved in the same cell development process, but are not able to complement for each other (contrary to what has been observed for the *P. falciparum* MAPKs (28)). This is consistent with our observation that Pfnek-2 and Pfnek-4 display distinct substrate specificity *in vitro* when classical exogenous substrates such as MBP, histone H1, or casein are used (Fig. 2*C*). Similarly, kinase assays using heat-inactivated parasite extracts as substrates consistently display different patterns of phosphorylated proteins depending on whether GST-Pfnek-2 or GST-Pfnek-4 is used in the reaction (data not shown). Thus, biochemical and reverse genetics data (absence of cross-complementation) concur to suggest that nek-2 and nek-4 fulfill non-redundant functions during meiosis. This, together with the fact that both enzymes are (i) active *in vitro* when expressed in *E. coli* as recombinant proteins, and (ii) essential for infection of the mosquito vector, is of considerable interest in the context of the search for targets for transmission-blocking intervention. The advantages of targeting more than one single target are well established (36), and the availability of enzymatic assays makes high throughput screening of chemical libraries on Pbnek-2 and Pbnek-4 a realistic possibility. The developmental effect of any hits can be tested in transmission experiments.

TABLE 1

***nek-2* is essential for transmission to the mosquito vector**

A. gambiae mosquitoes were fed on blood containing *P. falciparum* wild-type (3D7) or *pfnek-2*$^-$ (clone c9) gametocytes, and *A. stephensi* mosquitoes were fed on mice infected with wild-type and *pbnek-2*$^-$ *P. berghei* parasites. Midgut oocyst numbers were determined at days 10–12 after infection. Shown is the prevalence (mosquitoes with oocysts/total mosquitoes) and (in parentheses) the range of numbers of oocysts per midgut for the positive mosquitoes.

	Oocysts
P. falciparum	
Experiment 1	
3D7 wild-type	21/24 (1–7)
pfnek-2$^-$	1/36 (2)[a]
Experiment 2	
3D7 wild-type	15/22 (1–42)
pfnek-2$^-$	0/20 (0)
Experiment 3	
3D7 wild-type	10/20 (1–9)
pfnek-2$^-$	0/24 (0)
P. berghei	
Experiment 1	
Wild-type	20/20 (83–200)
pbnek-2$^-$	0/20
Experiment 2	
Wild-type	18/20 (52–200)
pbnek-2$^-$	0/20
Experiment 3	
Wild-type	20/20 (61–200)
pbnek-2$^-$	0/20

[a] The single mosquito infected with *pfnek-2*$^-$ gametocytes in experiment 1 contained 2 oocysts.

Acknowledgments—We are grateful to Pietro Alano for the gift of the anti-Pfg377 antiserum, and David Fidock and Geoff MacFadden for the pCAM BSD and pHGB/pCHD vectors, respectively. This work is based on gene identification made possible by the availability of the genome sequences of P. falciparum and P. berghei, and the PlasmoDB data base. We thank Dr. J. Chevalier (Service Scientifique de l'Ambassade de France à Londres) for continuing interest and support.

REFERENCES

1. Breman, J. G., Alilio, M. S., and Mills, A. (2004) *Am. J. Trop. Med. Hyg.* **71,** 1–15
2. Oakley, B. R., and Morris, N. R. (1983) *J. Cell Biol.* **96,** 1155–1158
3. Schultz, S. J., Fry, A. M., Sutterlin, C., Ried, T., and Nigg, E. A. (1994) *Cell Growth & Differ.* **5,** 625–635
4. Fry, A. M., Meraldi, P., and Nigg, E. A. (1998) *EMBO J.* **17,** 470–481
5. Davies, J. R., Osmani, A. H., De Souza, C. P., Bachewich, C., and Osmani, S. A. (2004) *Eukaryot. Cell* **3,** 1433–1444
6. O'Regan, L., Blot, J., and Fry, A. M. (2007) *Cell Div.* **2,** 25

7. Belham, C., Roig, J., Caldwell, J. A., Aoyama, Y., Kemp, B. E., Comb, M., and Avruch, J. (2003) *J. Biol. Chem.* **278,** 34897–34909
8. Ward, P., Equinet, L., Packer, J., and Doerig, C. (2004) *BMC Genomics* **5,** 79
9. Reininger, L., Billker, O., Tewari, R., Mukhopadhyay, A., Fennell, C., Dorin-Semblat, D., Doerig, C., Goldring, D., Harmse, L., Ranford-Cartwright, L., Packer, J., and Doerig, C. (2005) *J. Biol. Chem.* **280,** 31957–31964
10. Le Roch, K. G., Zhou, Y., Blair, P. L., Grainger, M., Moch, J. K., Haynes, J. D., De La Vega, P., Holder, A. A., Batalov, S., Carucci, D. J., and Winzeler, E. A. (2003) *Science* **301,** 1503–1508
11. Bahl, A., Brunk, B., Crabtree, J., Fraunholz, M. J., Gajria, B., Grant, G. R., Ginsburg, H., Gupta, D., Kissinger, J. C., Labo, P., Li, L., Mailman, M. D., Milgram, A. J., Pearson, D. S., Roos, D. S., Schug, J., Stoeckert, C. J., Jr., and Whetzel, P. (2003) *Nucleic Acids Res.* **31,** 212–215
12. Dorin, D., Le Roch, K., Sallicandro, P., Alano, P., Parzy, D., Poullet, P., Meijer, L., and Doerig, C. (2001) *Eur. J. Biochem.* **268,** 2600–2608
13. Lye, Y. M., Chan, M., and Sim, T. S. (2006) *FEBS Lett.* **580,** 6083–6092
14. Ringwald, P., Meche, F. S., Bickii, J., and Basco, L. K. (1999) *J. Clin. Microbiol.* **37,** 700–705
15. Carter, R., Ranford-Cartwright, L., and Alano, P. (1993) *Methods Mol. Biol.* **21,** 67–88
16. Tonkin, C. J., van Dooren, G. G., Spurck, T. P., Struck, N. S., Good, R. T., Handman, E., Cowman, A. F., and McFadden, G. I. (2004) *Mol. Biochem. Parasitol.* **137,** 13–21
17. Sidhu, A. B., Valderramos, S. G., and Fidock, D. A. (2005) *Mol. Microbiol.* **57,** 913–926
18. Mair, G. R., Braks, J. A., Garver, L. S., Wiegant, J. C., Hall, N., Dirks, R. W., Khan, S. M., Dimopoulos, G., Janse, C. J., and Waters, A. P. (2006) *Science* **313,** 667–669
19. Liu, J., Gluzman, I. Y., Drew, M. E., and Goldberg, D. E. (2005) *J. Biol. Chem.* **280,** 1432–1437
20. Rellos, P., Ivins, F. J., Baxter, J. E., Pike, A., Nott, T. J., Parkinson, D. M., Das, S., Howell, S., Fedorov, O., Shen, Q. Y., Fry, A. M., Knapp, S., and Smerdon, S. J. (2007) *J. Biol. Chem.* **282,** 6833–6842
21. de Koning-Ward, T. F., Olivieri, A., Bertuccini, L., Hood, A., Silvestrini, F., Charvalias, K., Berzosa Díaz, P., Camarda, G., McElwain, T. F., Papenfuss, T., Healer, J., Baldassarri, L., Crabb, B. S., Alano, P., and Ranford-Cartwright, L. C. (2008) *Mol. Microbiol.* **67,** 278–290
22. Alano, P., Read, D., Bruce, M., Aikawa, M., Kaido, T., Tegoshi, T., Bhatti, S., Smith, D. K., Luo, C., Hansra, S., Carter, R., and Elliott, J. F. (1995) *Mol. Biochem. Parasitol.* **74,** 143–156
23. Silvestrini, F., Alano, P., and Williams, J. L. (2000) *Parasitology* **121,** 465–471
24. Sinden, R. E., Canning, E. U., Bray, R. S., and Smalley, M. E. (1978) *Proc. R. Soc. Lond. B Biol. Sci.* **201,** 375–399
25. Motose, H., Tominaga, R., Wada, T., Sugiyama, M., and Watanabe, Y. (2008) *Plant J.* **54,** 829–844
26. Billker, O., Lindo, V., Panico, M., Etienne, A. E., Paxton, T., Dell, A., Rogers, M., Sinden, R. E., and Morris, H. R. (1998) *Nature* **392,** 289–292
27. Billker, O., Dechamps, S., Tewari, R., Wenig, G., Franke-Fayard, B., and Brinkmann, V. (2004) *Cell* **117,** 503–514
28. Dorin-Semblat, D., Quashie, N., Halbert, J., Sicard, A., Doerig, C., Peat, E., Ranford-Cartwright, L., and Doerig, C. (2007) *Mol. Microbiol.* **65,** 1170–1180
29. Arama, E., Yanai, A., Kilfin, G., Bernstein, A., and Motro, B. (1998) *Oncogene* **16,** 1813–1823
30. Rhee, K., and Wolgemuth, D. J. (1997) *Development* **124,** 2167–2177
31. Malumbres, M., and Barbacid, M. (2007) *Curr. Opin. Genet. Dev.* **17,** 60–65
32. Hayward, D. G., and Fry, A. M. (2006) *Cancer Lett.* **237,** 155–166
33. Palermo, G., Munné, S., and Cohen, J. (1994) *Hum. Reprod.* **9,** 1220–1225
34. Sathananthan, A. H., Kola, I., Osborne, J., Trounson, A., Ng, S. C., Bongso, A., and Ratnam, S. S. (1991) *Proc. Natl. Acad. Sci. U.S.A.* **88,** 4806–4810
35. Nagasato, C. (2005) *J. Plant Res.* **118,** 361–369
36. Zimmermann, G. R., Lehár, J., and Keith, C. T. (2007) *Drug Discov. Today* **12,** 34–42